Supplementary Information

Ionic liquid assisted high quality $MAPbBr_3$ Single Crystal growth for Photodetection Application

Apurba Mahapatra,[a,] Vishnu Anilkumar,[a] Joanna Kruszyńska,[a] Nada Mrkyvkova,[b,c] Peter Siffalovic,[b,c] Pankaj Yadav[d,e] and Daniel Prochowicz[a,]*

[a] Institute of Physical Chemistry, Polish Academy of Sciences, Kasprzaka 44/52, 01-224 Warsaw, Poland

[b] Institute of Physics, Slovak Academy of Sciences, Dubravska cesta 9, 84511 Bratislava, Slovakia.

[d] Center for Advanced Materials and Applications, Slovak Academy of Sciences, Dubravska cesta 9, 84511 Bratislava, Slovakia.

[d] Department of Solar Energy, School of Energy Technology, Pandit Deendayal Energy University, Gandhinagar-382 007, Gujarat, India.

[e] Department of Physics, School of Energy Technology, Pandit Deendayal Energy University, Gandhinagar-382 007, Gujarat, India.

Corresponding author: dprochowicz@ichf.edu.pl

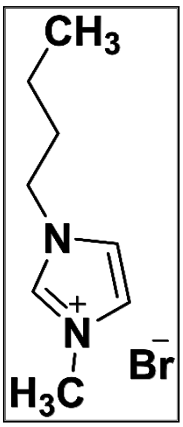

Figure S1. Molecular structure of BMIB IL.

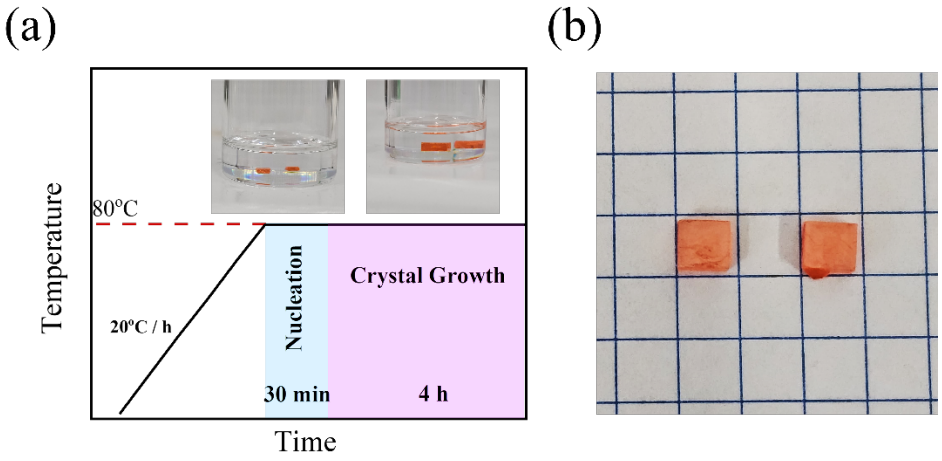

Figure S2. (a) Schematic representation of crystallization rate over time for $MAPbBr_3$ SCs using ITC method at 80°C. (b) Image of as-grown $MAPbBr_3$ SCs.

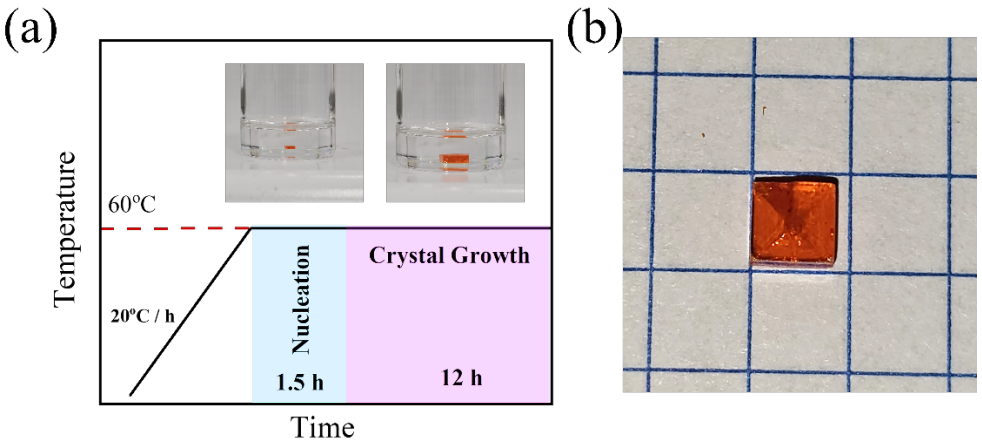

Figure S3. (a) Schematic representation of crystallization rate over time for $MAPbBr_3$ SCs using ITC method at 80°C. (b) Image of as-grown $MAPbBr_3$ SC in the presence of BMIB (5 %mol).

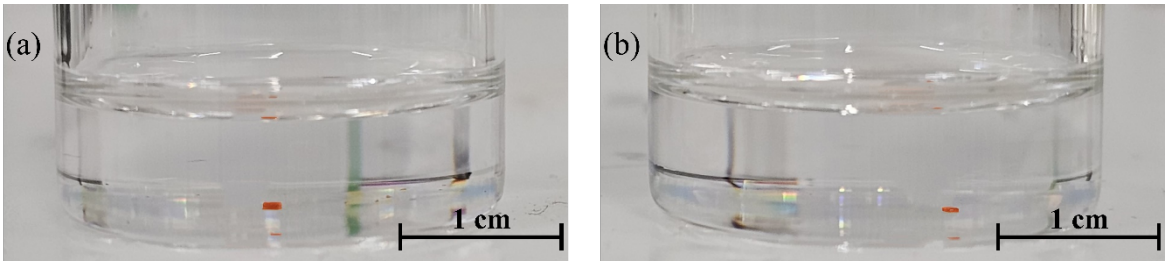

Figure S4. Photographs of $MAPbBr_3$ solution heated at 60°C for 12 h with (a) 1 mol% and (b) 3 mol% BMIB IL.

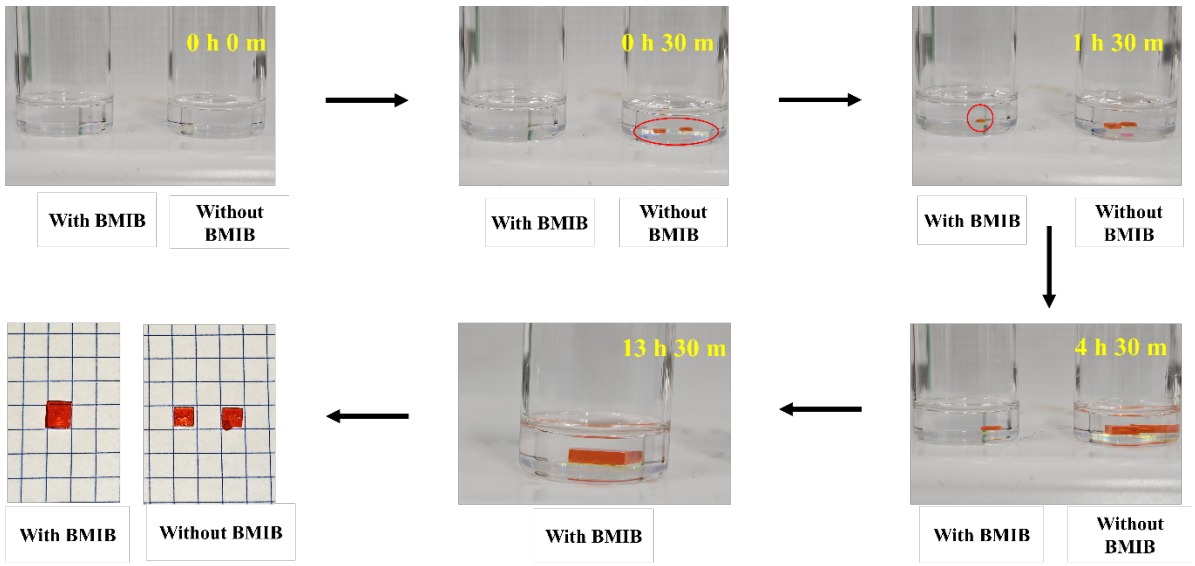

Figure S5. Image of crystallization process without and with 5 mol% BMIB IL at 80°C as a function of time.

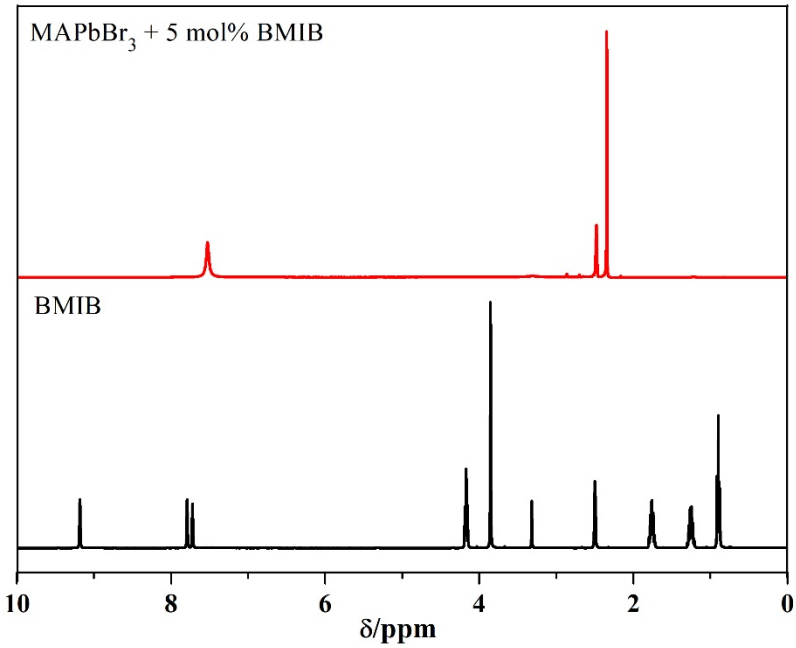

Figure S6. ^{1}H NMR spectrum of BMIB and $MAPbBr_3$ crystals with 5 mol% of BMIB measured in DMSO-d_6 solution.

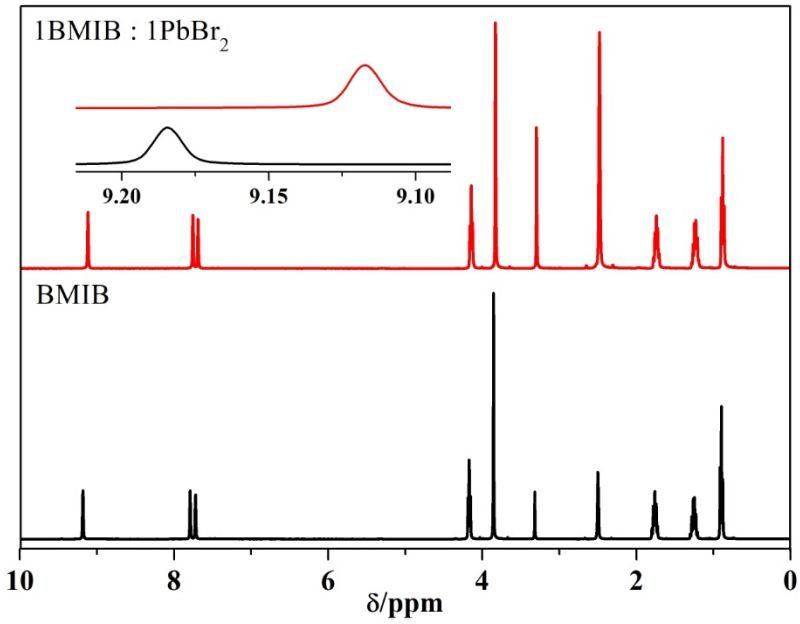

Figure S7. ^{1}H NMR spectrum of BMIB and mixture of BMIB : $PbBr_2$ (1:1) in DMSO-d_6 solution.

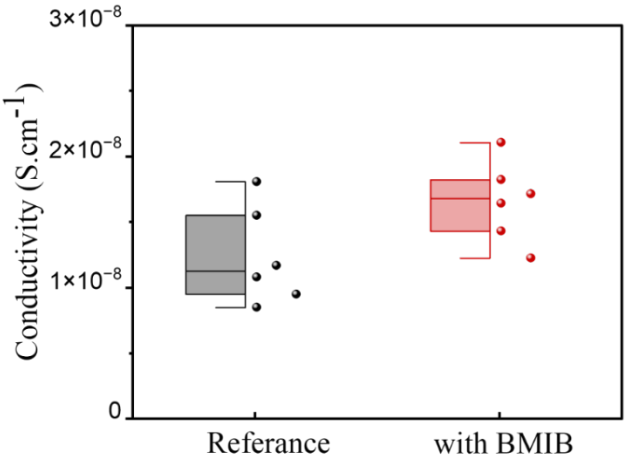

Figure S8. Conductivity of the reference and BMIB-based $MAPbBr_3$ SCs.

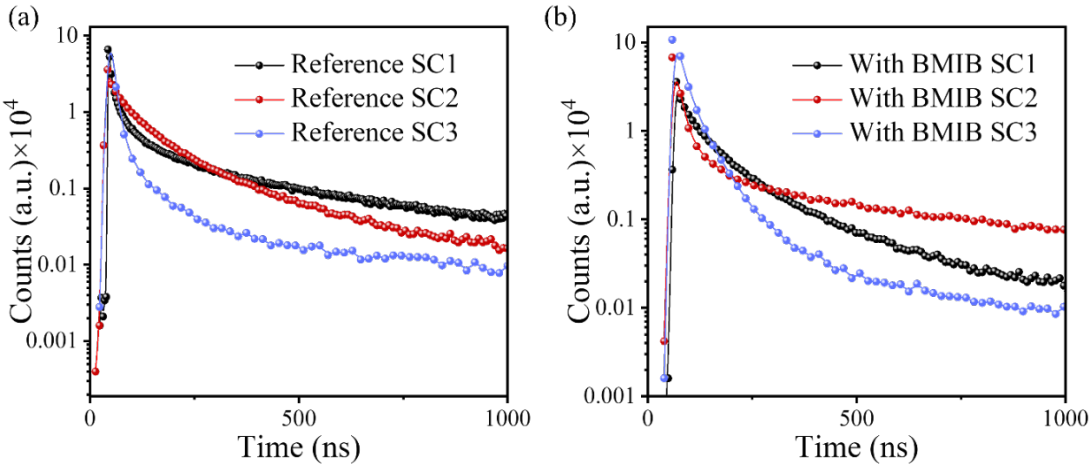

Figure S9. (a) Time-resolved photoluminescence (TRPL) of the three different reference and BMIB-based $MAPbBr_3$ SCs.

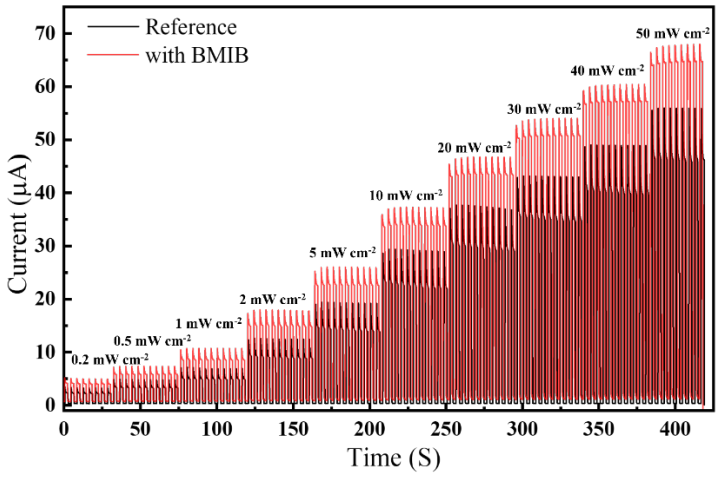

Figure S10. Intensity-dependent transient photoresponse of the reference $MAPbBr_3$ SC-based PD and BMIB-based PD under light pulse.

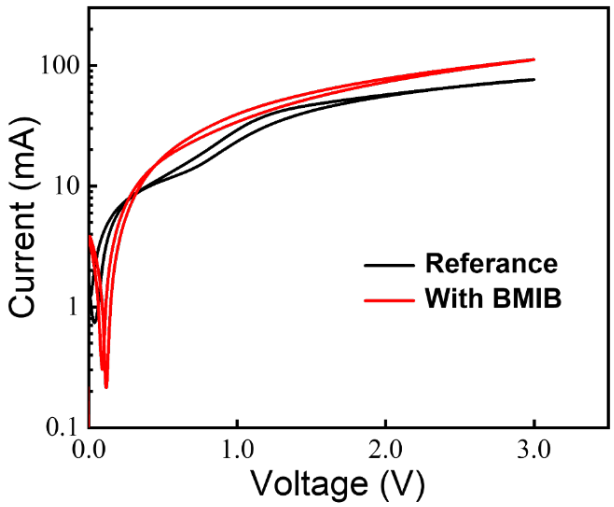

Figure S11. *I*−*V* characteristics at 50 W cm^{-2} in forward and reverse scan directions for both the $MAPbBr_3$ SC-based PD. Scan rate: 100 mV s^{-1}.

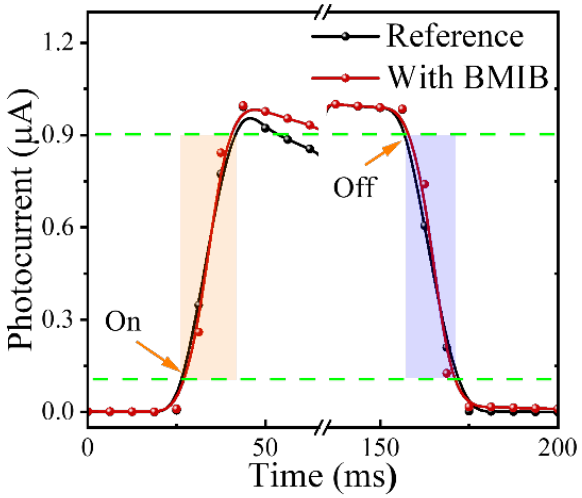

Figure S12. Response speed of the reference and BMIB-based PDs at 1 mW cm^{-2} irradiance power of green light (530 nm) at 2 V.

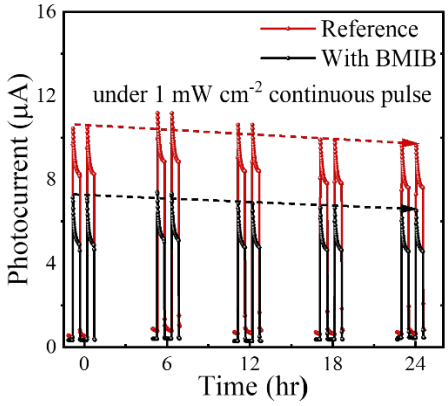

Figure S13. Functional stability of the reference and BMIB-based PDs under 1 mW cm^{-2} irradiance power of green light (530 nm) at 2 V.

Table S1. Comparison of nucleation time and growth time of $MAPbBr_3$ SCs.

Methods	Temperature	Nucleation time	SCs / growth time
without (reference)	60 °C	N/A	NA / 12 h
	80 °C	30 min	Large SCs / 4h
with BMIB 1 mol%	60 °C	5 h	Small SCs / 24 h
with BMIB 3 mol%	60 °C	4 h	Small SCs / 24 h
with BMIB 5 mol%	60 °C	90 min	Large SCs / 12h
with BMIB 10 mol%	60 °C	N/A	NA / 12 h

Table S2. Average growth rate of $MAPbBr_3$ SCs.

Methods	Temperature	Nucleation time	Collected SCs weight after 6h growth time	Average growth rate
without (reference)	80 °C	30 min	397	1.1 mg / min
with BMIB 5%		60 min	286 mg	0.8 mg / min

Table S3. Calculated lattice strain of reference and (b) BMIB-based $MAPbBr_3$ SCs.

peak position 2θ (deg)	FWHM (deg)		lattice strain (%)	
	without (reference)	with BMIB 5 mol%	without (reference)	with BMIB 5 mol%
14.98	0.30	0.19	0.996	0.631
30.22	0.29	0.23	0.469	0.372
45.99	0.41	0.24	0.422	0.247

Table S4. The comparison of the performance parameters for pure $MAPbBr_3$ SC based PDs growth by ITC and our work.

Device	Growth temp. (°C)	Seeded /Additive	Duration	Wavelength (nm) / Bias (V)	R (AW^{-1})	D* Jones	EQE (%) /Gain	On/off time	Ref
Pt/$MAPbBr_3$/Pt	80	-	4h	448 nm 2 V	1.99	5.09×10^{12}	553		[1]
Cr/$MAPbBr_3$/Au	60	-	20 days	515 nm 5 V	55.7	8×10^{13}	13453	120 ms / 86 ms	[2]
Pt/$MAPbBr_3$/Pt	110	-	-	White light 2V	0.059	-	-	<20 ns / 500 µs	[3]

Au/MAPbBr$_3$/Au	80	-	-	350 nm	-	-	900	-/ 30 µs	4
Au/MAPbBr$_3$/Au	85	seeded	-	405 nm 9.84 V	0.038 (110)	-	0.113 (110)	0.153 s / 0.057 s	5
Au/MAPbBr$_3$/Au	80	-	-	576 nm 2 V	5.3	7.4×10^{11}	1130	3.90 ms / 4.09 ms	6
C/MAPbBr$_3$/C	65	Seeded	6 h	473 nm 5 V	5.49	5.35×10^{11}			7
Pt/MAPbBr$_3$/Pt	80	-	4 h	530 nm 2V	3.5	7.8×10^{12}	839	14.3 ms / 16.1 ms	This work
	60	BMIB IL	12 h	530 nm 2V	4.81	9.35×10^{12}	1124	12.1 ms / 14.8 ms	

Supplementary Note 1. The lattice strain from XRD was calculated by using the HighScore analysis software from PANanalytical. The lattice strain (%) is calculated by the tangent formula:

$$lattice\ strain = \frac{B_{struct}}{4\tan\theta} \qquad \text{(S1)}$$

where, B_{struct} describes the structural broadening by:

$$B_{struct} = \sqrt{{B_{obs}}^2 - {B_{std}}^2} \qquad \text{(S2)}$$

where, B_{obs} *and* B_{std} are breadth obtained from the sample to be analyzed and breadth obtained from the standard sample, respectively. [8]

Supplementary Note 2.

Responsivity (R), Specific Detectivity (D*) and External Quantum Efficiency (EQE) are important parameters for a PD. The photoresponse (R) of the PD, was calculated using the formula:[1]

$$R = (J_{ph} - J_d)/P \qquad (S3)$$

where the J_{ph} is the photocurrent density, J_d is the dark current density, and P is the illumination power. The D* of the PD, was calculated by the equation; [1]

$$D^* = R/\sqrt{(2qJ_d)} \qquad (S4)$$

where, q is the charge of electron.

The EQE of the PDs were calculated by; [1]

$$EQE = Rhc/e\lambda \qquad (S5)$$

The Rise time are calculated from time taken to reach 10% to 90% of the photocurrent value after switch on light and fall-time are calculated from time taken to decay 90% to 10% of the photocurrent value after switch off light of a PDs (extracted from the normalized photocurrents).[9]

References

(1) Mahapatra, A.; Anilkumar, V.; Chavan, R. D.; Yadav, P.; Prochowicz, D. Understanding the Origin of Light Intensity and Temperature Dependence of Photodetection Properties in a $MAPbBr_3$ Single-Crystal-Based Photoconductor. *ACS Photonics* **2023**, *10*, 1424–1433.

(2) Liu, Y.; Zhang, Y.; Yang, Z.; Feng, J.; Xu, Z.; Li, Q.; Hu, M.; Ye, H.; Zhang, X.; Liu, M.; Zhao, K.; Liu, S. Low-Temperature-Gradient Crystallization for Multi-Inch High-Quality Perovskite Single Crystals for Record Performance Photodetectors. *Mater. Today* **2019**, *22*, 67–75.

(3) Cho, Y.; Jung, H. R.; Kim, Y. S.; Kim, Y.; Park, J.; Yoon, S.; Lee, Y.; Cheon, M.; Jeong, S. Y.; Jo, W. High Speed Growth of $MAPbBr_3$ Single Crystals via Low-Temperature Inverting Solubility: Enhancement of Mobility and Trap Density for Photodetector Applications. *Nanoscale* **2021**, *13*, 8275–8282.

(4) Wang, X.; Huang, Y.; Lei, W.; Li, Q.; Zhang, X.; Khan, Q.; Wang, B.; Wang, X.; Huang, Y.; Lei, W.; Li, Q.; Zhang, X.; Khan, Q.; Wang, B. Asymmetrical Photodetection Response of Methylammonium Lead Bromide Perovskite Single Crystal. *Cryst. Res. Technol.* **2017**, *52*, 1700115.

(5) Zuo, Z.; Ding, J.; Zhao, Y.; Du, S.; Li, Y.; Zhan, X.; Cui, H. Enhanced Optoelectronic Performance on the (110) Lattice Plane of an $MAPbBr_3$ Single Crystal. *J. Phys. Chem. Lett.* **2017**, *8*, 684–689.

(6) Gavranovic, S.; Pospisil, J.; Zmeskal, O.; Novak, V.; Vanysek, P.; Castkova, K.; Cihlar, J.; Weiter, M. Electrode Spacing as a Determinant of the Output Performance of Planar-Type Photodetectors Based on Methylammonium Lead Bromide Perovskite Single Crystals. *ACS Appl. Mater. Interfaces* **2022**, *14*, 20159–20167.

(7) Zia, W.; Aranda, C. A.; Pospisil, J.; Kovalenko, A.; Rai, M.; Momblona, C.; Gorji, S.; Muñoz-Matutano, G.; Saliba, M. Impact of Low-Temperature Seed-Assisted Growth on the Structural and Optoelectronic Properties of $MAPbBr_3$ Single Crystals. *Chem. Mater.* **2023**, *35*, 5458–5467.

(8) Amari, S.; Verilhac, J. M.; Gros D'Aillon, E.; Ibanez, A.; Zaccaro, J. Optimization of the Growth Conditions for High Quality CH3NH3PbBr3 Hybrid Perovskite Single Crystals. *Cryst. Growth Des.* **2020**, *20*, 1665–1672.

(9) Mahapatra, A.; Prochowicz, D.; Kruszyńska, J.; Satapathi, S.; Akin, S.; Kumari, H.; Kumar, P.; Fazel, Z.; Tavakoli, M. M.; Yadav, P. Effect of Bromine Doping on the Charge Transfer, Ion Migration and Stability of the Single Crystalline $MAPb(Br_xI_{1-x})_3$ Photodetector. *J. Mater. Chem. C* **2021**, *9*, 15189–15200.